Chapter 26

Decoupling

An idealized requirement in MIMO control-system design is that of decoupling. If a plant is dynamically decoupled, then changes in the set-point of one process variable lead to a response in that process variable but *all other* process variables remain constant. The advantages of such a design are intuitively clear: e.g., a temperature may be required to be changed, but it may be undesirable for other variables (*e.g., pressure*) to suffer any associated transient. Full dynamic decoupling is a very stringent requirement. Thus, in practice, it is more usual to seek dynamic decoupling over some desired bandwidth.

This chapter describes the design procedures necessary to achieve dynamic decoupling. In particular, we discuss

- *dynamic decoupling for stable minimum-phase systems*
- *dynamic decoupling for stable nonminimum-phase systems*
- *dynamic decoupling for open-loop unstable systems*

As might be expected, full dynamic decoupling is a strong requirement and is generally not cost-free. We will thus also quantify the performance cost of decoupling by using frequency-domain procedures. These allow a designer to assess *a-priori* whether the cost associated with decoupling is acceptable in a given application.

Of course, some form of decoupling is a very common requirement. For example, static decoupling is almost always a design requirement. The question then becomes, over what bandwidth will decoupling (*approximately*) be asked for? It will turn out that the additional cost of decoupling is a function of open-loop poles and zeros in the right-half plane. Thus if one is restricting decoupling in some bandwidth, then by focusing attention on those open-loop poles and zeros that fall within this bandwidth, one can get a feel for the cost of decoupling over that bandwidth.

We will also examine the impact of actuator saturation on decoupling. In the case of static decoupling, it is necessary to avoid integrator wind-up. This can be achieved by using methods that are analogous to the SISO case treated in Chapter 11.

Stable Systems

We first consider the situation in which the open-loop poles of the plant are located in desirable locations. We will employ the affine-parameterization technique described in Chapter 25 to design a controller that achieves full dynamic decoupling.

Stable Systems: Part 1 - Minimum-Phase Case

We refer to the general Q-design procedure outlined in Chapter 25.

To achieve dynamic decoupling, we make the following choice for $\mathbf{Q}(s)$.

$$\mathbf{Q}(s) = \boldsymbol{\xi}_{\mathbf{R}}(s)[\boldsymbol{\Lambda}_{\mathbf{R}}(s)]^{-1}\mathbf{D}_{\mathbf{Q}}(s)$$

$$\boldsymbol{\Lambda}_{\mathbf{R}}(s) = \mathbf{G}_{\mathbf{o}}(s)\boldsymbol{\xi}_{\mathbf{R}}(s)$$

$$\mathbf{D}_{\mathbf{Q}}(s) = \text{diag}\left(\frac{1}{p_1(s)}, \frac{1}{p_2(s)}, \cdots, \frac{1}{p_m(s)}\right)$$

Where $\boldsymbol{\xi}_{\mathbf{R}}(s)$ is the right interactor, and $p_1(s)$, $p_2(s)$, … $p_m(s)$ are stable polynomials chosen to make $\mathbf{Q}(s)$ proper. The polynomials $p_1(s)$, $p_2(s)$, … $p_m(s)$ should be chosen to have unit d.c. gain.

We observe that, with the above choice, we achieve the following nominal complementary sensitivity:

$$\begin{aligned}
\mathbf{T_o}(s) &= \mathbf{G_o}(s)\mathbf{Q}(s) \\
&= \mathbf{G_o}(s)\boldsymbol{\xi}_{\mathbf{R}}(s)[\boldsymbol{\Lambda}_{\mathbf{R}}(s)]^{-1}\mathbf{D_Q}(s) \\
&= \mathbf{G_o}(s)\boldsymbol{\xi}_{\mathbf{R}}(s)[\mathbf{G_o}(s)\boldsymbol{\xi}_{\mathbf{R}}(s)]^{-1}\mathbf{D_Q}(s) \\
&= \text{diag}\left(\frac{1}{p_1(s)}, \frac{1}{p_2(s)}, \cdots, \frac{1}{p_m(s)}\right)
\end{aligned}$$

We see that this is diagonal, as required. The associated control-system structure would then be as shown below:

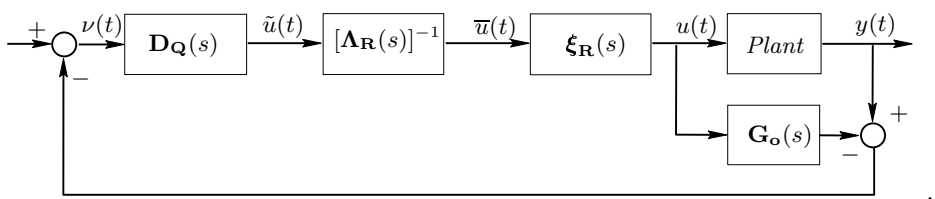

Figure 26.1: *IMC decoupled control of stable MIMO plants*

Actually, the above design is not unique. For example, an alternative choice for $\mathbf{Q}(s)$ is

$$\mathbf{Q}(s) = [\mathbf{\Lambda_L}(s)]^{-1}\boldsymbol{\xi}_{\mathbf{L}}(s)\mathbf{D_Q}(s)$$

where $\mathbf{D_Q}(s)$ is given by

$$\mathbf{D_Q}(s) = diag\left(\frac{1}{p_1(s)}, \frac{1}{p_2(s)}, \cdots, \frac{1}{p_m(s)}\right)$$

Note also that $\mathbf{D_Q}(s)$ can have the more general structure

$$\mathbf{D_Q}(s) = \text{diag}\,(t_1(s), t_2(s), \cdots, t_m(s))$$

where $t_1(s)$, $t_2(s)$, …, $t_m(s)$ are proper stable transfer functions having relative degrees equal to the corresponding column degrees of the left interactor for $\mathbf{G_o}(s)$. The transfer functions $t_1(s)$, $t_2(s)$, …, $t_m(s)$ should be chosen to have unit d.c. gain.

Example 26.1

Consider a stable 2×2 MIMO system having the nominal model

$$\mathbf{G_o}(s) = \frac{1}{(s+1)^2(s+2)} \begin{bmatrix} 2(s+1) & -1 \\ (s+1)^2 & (s+1)(s+2) \end{bmatrix}$$

Choose a suitable matrix $\mathbf{Q}(s)$ to control this plant, using the affine parameterization, in such a way that the MIMO control loop is able to track references of bandwidths less than or equal to 2[rad/s] and 4[rad/s] in channels 1 and 2, respectively.

We will aim to obtain a complementary sensitivity matrix given by

$$\mathbf{T_o}(s) = \mathrm{diag}(T_{11}(s), T_{22}(s))$$

where $\mathbf{T}_{11}(s)$ and $\mathbf{T}_{22}(s)$ will be chosen to have bandwidths 2[rad/s] and 4[rad/s] in channels 1 and 2, respectively.

Then, $\mathbf{Q}(s)$ must ideally satisfy

$$\mathbf{Q}(s) = [\mathbf{G_o}(s)]^{-1}\mathbf{T_o}(s).$$

We choose the structure $\mathbf{Q}(s) = [\mathbf{\Lambda_L}(s)]^{-1}\boldsymbol{\xi}_\mathbf{L}(s)\mathbf{D_Q}(s)$ from which we see that $\mathbf{T_o}(s) = \mathbf{D_Q}(s)$. Hence the relative degrees of $\mathbf{T}_{11}(s)$ and $\mathbf{T}_{22}(s)$ will be chosen equal to the degrees of the first and second column of the left interactor for $\mathbf{G_o}(s)$, respectively.

The left interactor $\boldsymbol{\xi_L}(s)$ is

$$\boldsymbol{\xi_L}(s) = \mathrm{diag}\big((s+\alpha)^2, (s+\alpha)\big); \qquad \alpha \in \mathsf{R}^+$$

Then

$$\mathbf{Q}(s) = [\boldsymbol{\xi_L}(s)\mathbf{G_o}(s)]^{-1}\boldsymbol{\xi_L}(s)\mathbf{T_o}(s).$$

Hence, $\mathbf{Q}(s)$ is proper if and only if $\mathbf{T_o}(s)$ is chosen so as to make $\boldsymbol{\xi}_\mathbf{L}(s)\mathbf{T_o}(s)$ proper.

Thus, possible choices for $\mathbf{T}_{11}(s)$ and $\mathbf{T}_{22}(s)$ are

$$T_{11}(s) = \frac{4}{s^2 + 3s + 4}; \qquad \text{and} \qquad T_{22}(s) = \frac{4(s+4)}{s^2 + 6s + 16}$$

To obtain the final expression for $\mathbf{Q}(s)$, we next need to compute $[\mathbf{G_o}(s)]^{-1}$, which is given by

$$[\mathbf{G_o}(s)]^{-1} = \frac{s+2}{2s+5}\begin{bmatrix}(s+1)(s+2) & 1\\ -(s+1)^2 & 2(s+1)\end{bmatrix}$$

We finally obtain

$$\mathbf{Q}(s) = [\mathbf{G_o}(s)]^{-1}\mathbf{T_o}(s) = \frac{s+2}{2s+5}\begin{bmatrix} \dfrac{4(s+1)(s+2)}{s^2+3s+4} & \dfrac{4(s+4)}{s^2+6s+16} \\ \dfrac{-4(s+1)^2}{s^2+3s+4} & \dfrac{8(s+4)(s+1)}{s^2+6s+16} \end{bmatrix}$$

The above design procedure is limited to minimum-phase systems. In particular, it is clear that $\mathbf{Q}(s)$, chosen as above, is stable if and only if $\mathbf{G_o}(s)$ is minimum phase, because $[\mathbf{\Lambda_R}(s)]^{-1}$ and $[\mathbf{\Lambda_L}(s)]^{-1}$ involve an inverse of $\mathbf{G_o}(s)$. We therefore need to modify $\mathbf{Q}(s)$ so as to ensure stability when $\mathbf{G_o}(s)$ is nonminimum phase. A way of doing this is described below.

Stable Systems: Part 2 - Nonminimum-Phase Case

We will begin with the state space realization for $[\mathbf{\Lambda_R}(s)]^{-1}$, defined by a 4-tuple $(\mathbf{A}_\lambda, \mathbf{B}_\lambda, \mathbf{C}_\lambda, \mathbf{D}_\lambda)$. We will denote by $\tilde{u}(t)$ the input to this system. Our aim is to modify $[\mathbf{\Lambda_R}(s)]^{-1}$ so as to achieve two objectives:

(*i*) render the transfer function stable, whilst;

(*ii*) retaining its diagonalizing properties.

To this end, we define the following subsystem, which is driven by the i^{th} component of $\tilde{u}(t)$

$$\dot{x}_i(t) = \mathbf{A_i} x_i(t) + \mathbf{B_i} \tilde{u}_i(t)$$
$$\upsilon_i(t) = \mathbf{C_i} x_i(t) + \mathbf{D_i} \tilde{u}_i(t)$$

where $\upsilon_i(t) \in \mathbb{R}^m$, $\tilde{u}_i(t) \in \mathbb{R}$, and $(\mathbf{A_i}, \mathbf{B_i}, \mathbf{C_i}, \mathbf{D_i})$ is a minimal realization of the transfer function from the i^{th} component of $\tilde{u}(t)$ to the complete vector output $\bar{u}(t)$. Thus $(\mathbf{A_i}, \mathbf{B_i}, \mathbf{C_i}, \mathbf{D_i})$ is a minimal realization of $(\mathbf{A}_\lambda, \mathbf{B}_\lambda e_i, \mathbf{C}_\lambda, \mathbf{D}_\lambda e_i)$, where e_i is the i^{th} column of the $m \times m$ identity matrix.

We next apply stabilizing state feedback to each of these subsystems - i.e., we form

$$\tilde{u}_i(t) = -\mathbf{K_i} x_i(t) + \overline{r}_i(t); \qquad i = 1, 2, \ldots, m$$

where $\bar{r}_i(t) \in \mathbb{R}$. The design of $\mathbf{K_i}$ can be done in any convenient fashion - e.g., by linear quadratic optimization.

Finally we add together the m vectors $\upsilon_1(t)$, $\upsilon_2(t)$, … $\upsilon_m(t)$ to produce an output, which can be renamed $\bar{u}(t)$:

$$\overline{u}(t) = \sum_{i=1}^{m} \upsilon_i(t)$$

We then have the following result:

Lemma 26.1:

(*a*) The transfer function from $\bar{r}(t) = [\bar{r}_1(t)\,\bar{r}_2(t)\cdots\bar{r}_m(t)]^T$ to $\bar{u}(t)$ is given by

$$\mathbf{W}(s) = [\mathbf{\Lambda_R}(s)]^{-1}\,\mathbf{D_z}(s)$$

where

$$[\Lambda_R(s)]^{-1} = (C_\lambda[s\mathbf{I} - A_\lambda]^{-1}B_\lambda + D_\lambda)$$
$$\mathbf{D_z}(s) = diag\left\{[1 + \mathbf{K_i}[s\mathbf{I} - \mathbf{A_i}]^{-1}\mathbf{B_i}]^{-1}\right\}$$

(*b*) $\mathbf{\Lambda_R}(s)\mathbf{W}(s)$ is a diagonal matrix.

(*c*) $\mathbf{W}(s)$ has a state space realization as described above.

Proof: See the book.

Returning now to the problem of determining Q(s), we choose

$$\mathbf{Q}(s) = \boldsymbol{\xi}_{\mathbf{R}}(s)\mathbf{W}(s)\mathbf{D}_{\mathbf{Q}}(s)$$

This is equivalent to

$$\mathbf{Q}(s) = \boldsymbol{\xi}_{\mathbf{R}}(s)[\boldsymbol{\xi}_{\mathbf{R}}(s)]^{-1}[\mathbf{G}_{\mathbf{o}}(s)]^{-1}\mathbf{D}_{\mathbf{z}}(s)\mathbf{D}_{\mathbf{Q}}(s)$$

Then

$$\mathbf{Q}(s) = [\mathbf{G}_{\mathbf{o}}(s)]^{-1}\mathbf{D}_{\mathbf{z}}(s)\,\mathrm{diag}\,\{t_1(s), t_2(s), \cdots, t_m(s)\}$$

Finally, we see that the resulting nominal complementary sensitivity is

$$\mathbf{T_o}(s) = \mathrm{diag}\left\{[1 + \mathbf{K_i}[s\mathbf{I} - \mathbf{A_i}]^{-1}\mathbf{B_i}]^{-1} t_i(s)\right\}$$

Note this complementary sensitivity is achieved without requiring any unstable pole-zero cancellations, and that any nonminimum-phase zeros in the plant are retained in $\mathbf{T_o}(s)$, which is a requirement for internal stability.

The reader will notice that it is implicit in the above design that some of the NMP zeros have been duplicated and appear in multiple diagonal elements. At worst, each NMP zero will appear in every diagonal term. Precisely how many zeros will appear and in which channel, depends on the degree of each minimum realization involved.

This *spreading* of NMP zeros is one of the costs associated with demanding full diagonal decoupling.

Decoupling Invariants

Actually, the NMP zeros appearing in

$$\mathbf{T_o}(s) = \mathrm{diag}\left\{[1 + \mathbf{K_i}[s\mathbf{I} - \mathbf{A_i}]^{-1}\mathbf{B_i}]^{-1} t_i(s)\right\}$$

are diagonalizing invariants and appear in *all possible* diagonalized closed loops. Thus, spreading NMP dynamics into other channels is a trade-off inherently associated with decoupling.

The final implementation of **Q**(s) is as shown below.

Figure 26.2: *Diagonal decoupling MIMO controller (Q(s))*

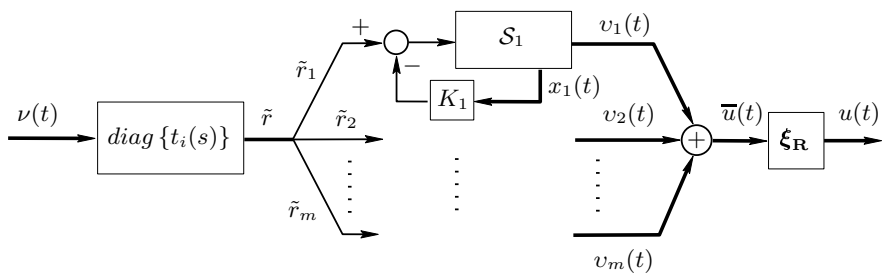

Example 26.2

Consider a plant having the nominal model

$$\mathbf{G_o}(s) = \frac{1}{(s+1)^2}\begin{bmatrix} s+2 & -3 \\ -2 & 1 \end{bmatrix}$$

This model has a NMP zero at $s = 4$. To synthesize a controller following the ideas presented above, we first compute a right interactor matrix, which turns out to have the general form $\boldsymbol{\xi}_{\mathbf{R}}(s) = \text{diag}\{s + \alpha, (s + \alpha)^2\}$. For numerical simplicity, we choose $\alpha = 1$. Then

$$[\boldsymbol{\Lambda}_{\mathbf{R}}(s)]^{-1} = [\mathbf{G}_{\mathbf{o}}(s)\boldsymbol{\xi}_{\mathbf{R}}(s)]^{-1} = \frac{1}{s-4}\begin{bmatrix} s+1 & 3(s+1) \\ 2 & s+2 \end{bmatrix}$$

and a state space realization for $[\boldsymbol{\Lambda}_{\mathbf{R}}(s)]^{-1}$ is

$$\mathbf{A} = \begin{bmatrix} 4 & 0 \\ 0 & 4 \end{bmatrix}; \quad \mathbf{B} = \mathbf{I}; \quad \mathbf{C} = \begin{bmatrix} 5 & 15 \\ 2 & 6 \end{bmatrix}; \quad \mathbf{D} = \begin{bmatrix} 1 & 3 \\ 0 & 1 \end{bmatrix}$$

We next compute ($\mathbf{A_i}$, $\mathbf{B_i}$, $\mathbf{C_i}$, $\mathbf{D_i}$) as a minimal realization of ($\mathbf{A}_\lambda$, $\mathbf{B}_\lambda e_i$, $\mathbf{C}_\lambda$, $\mathbf{D}_\lambda e_i$), for $i = 1$, $i = 2$. This computation yields

$$\mathbf{A_1} = 4 \qquad \mathbf{B_1} = 1 \qquad \mathbf{C_1} = [5 \quad 2]^T \qquad \mathbf{D_1} = [1 \quad 0]^T$$

$$\mathbf{A_2} = 4 \qquad \mathbf{B_2} = 1 \qquad \mathbf{C_2} = [15 \quad 6]^T \qquad \mathbf{D_2} = [3 \quad 1]^T$$

These subsystems can be stabilized by state feedback with gains $\mathbf{K_1}$ and $\mathbf{K_2}$, respectively. For this case, each gain is chosen to shift the unstable pole at $s = 4$ to a stable location, say $s = -10$, which leads to $\mathbf{K_1} = \mathbf{K_2} = 14$. Thus, $\mathbf{D_z}(s)$ is a 2×2 diagonal matrix given by

$$\mathbf{D_z}(s) = \frac{s-4}{s+10}\,\mathbf{I}$$

We finally choose $\mathbf{D_Q}(s)$ to achieve a bandwidth approximately equal to 3[rad/s], say

$$\mathbf{D_Q}(s) = \text{diag}\left\{ \frac{-9(s+10)}{4(s^2+4s+9)} \quad \frac{-90}{4(s^2+4s+9)} \right\}$$

Note that the elements $t_1(t)$ and $t_2(s)$ in $\mathbf{D_Q}(s)$ have been chosen of relative degree equal to the corresponding column degrees of the interactor $\boldsymbol{\xi}_{\mathbf{R}}(s)$. Also, their d.c. gains have been chosen to yield unit d.c. gain in the complementary sensitivity $\mathbf{T_o}(s)$, leading to

$$\mathbf{T_o}(s) = \text{diag}\left\{ \frac{-9(s-4)}{4(s^2+4s+9)} \quad \frac{-90(s-4)}{4(s+10)(s^2+4s+9)} \right\}$$

Pre- and PostDiagonalization

The transfer-function matrix $\mathbf{Q}(s)$ presented in

$$\mathbf{Q}(s) = \boldsymbol{\xi}_{\mathbf{R}}(s)\mathbf{W}(s)\mathbf{D}_{\mathbf{Q}}(s)$$

is actually a right-diagonalizing compensator for a stable (*but not necessarily minimum-phase*) plant. This can be seen by noting that

$$\mathbf{G_o}(s)\boldsymbol{\Pi}_{\mathbf{R}}(s) = \operatorname{diag}\left\{[1 + \mathbf{K_i}[s\mathbf{I} - \mathbf{A_i}]^{-1}\mathbf{B_i}]^{-1}t_i(s)\right\}$$

where

$$\begin{aligned}\boldsymbol{\Pi}_{\mathbf{R}}(s) &= \mathbf{Q}(s) \\ &= \boldsymbol{\xi}_{\mathbf{R}}(s)\mathbf{W}(s)\mathbf{D}_{\mathbf{Q}}(s)\end{aligned}$$

It is sometimes also desirable to have a left-diagonalizing compensator. We could derive such a compensator from first principles. However, a simple way is to first form

$$\overline{\mathbf{G}}_{\mathbf{o}}(s) = \mathbf{G}_{\mathbf{o}}^{\mathbf{T}}(s)$$

We find a right-diagonalizing compensator $\overline{\Pi}_{\mathbf{R}}(s)$ for $\overline{\mathbf{G}}_{\mathbf{o}}(s)$ by using the method outlined above. We then let $\Pi_{\mathbf{L}}(s) = \overline{\Pi}_{\mathbf{R}}(s)^T$, which has the following property.

$$\mathbf{\Pi_L}(s)\mathbf{G_o}(s) = \overline{\mathbf{\Pi}}_{\mathbf{R}}^{\mathbf{T}}(s)\overline{\mathbf{G}}_{\mathbf{o}}(s)^T = [\overline{\mathbf{G}}_{\mathbf{o}}(s)\mathbf{\Pi_R}(s)]^T$$

Which is a diagonal matrix by construction.

Unstable Systems

We next turn to the problem of designing a decoupling controller for an unstable MIMO plant. Here we have an additional complexity: some minimal feedback is necessary to ensure stability. To gain insight into this problem, we describe four alternative design choices in the book; namely

(*i*) a two-degree-of-freedom design based on prefiltering the reference;

(*ii*) a two-degree-of-freedom design using the affine parameterization;

(*iii*) a design based on one-degree-of-freedom state feedback; and

(*iv*) a design integrating both state feedback and the affine parameterization.

Two-Degree-of-Freedom Design Based on PreFiltering the Reference

If one requires full dynamic decoupling for reference-signal changes only, then this can be readily achieved by first stabilizing the system by using some suitable controller $C(s)$ and then using prefiltering of the reference signal. The essential idea is illustrated on the next slide.

Figure 26.3: *Prefilter design for full dynamic decoupling*

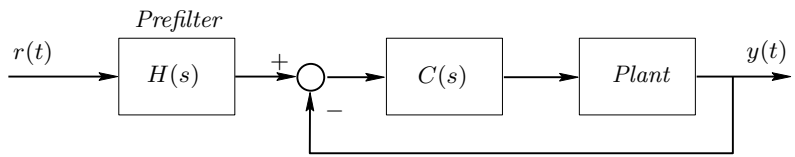

Say that the plant has transfer function $\mathbf{G_o}(s)$; then the closed-loop transfer function linking $R(s)$ to $Y(s)$ is

$$\mathbf{G_{cl}}(s) = \left[\mathbf{I} + \mathbf{G_o}(s)\mathbf{C}(s)\right]^{-1}\mathbf{G_o}(s)\mathbf{C}(s)\mathbf{H}(s)$$

To achieve decoupling, one then need only choose $\mathbf{H}(s)$ as a right-diagonalizing precompensator for the stable transfer function $[\mathbf{I} + \mathbf{G_o}(s)\mathbf{C}(s)]^{-1}\mathbf{G_o}(s)\mathbf{C}(s)$.

Example 26.4

Consider the plant

$$\mathbf{G_o}(s) = \mathbf{G_{oN}}(s)[\mathbf{G_{oD}}(s)]^{-1}$$

where

$$\mathbf{G_{oN}}(s) = \begin{bmatrix} -5 & s^2 \\ 1 & -0.0023 \end{bmatrix}; \qquad \mathbf{G_{oD}}(s) = \begin{bmatrix} 25s+1 & 0 \\ 0 & s(s+1)^2 \end{bmatrix}$$

The state space model for the system is

$$\dot{x}_p(t) = \mathbf{A_o} x_p(t) + \mathbf{B_o} u(t)$$
$$y(t) = \mathbf{C_o} x_p(t) + \mathbf{D_o} u(t)$$

where

$$\mathbf{A_o} = \begin{bmatrix} -0.04 & 0 & 0 & 0 \\ 0 & -2 & -1 & 0 \\ 0 & 1 & 0 & 0 \\ 0 & 0 & 1 & 0 \end{bmatrix} \qquad \mathbf{B_o} = \begin{bmatrix} 1 & 0 \\ 0 & 1 \\ 0 & 0 \\ 0 & 0 \end{bmatrix}$$

$$\mathbf{C_o} = \begin{bmatrix} -0.2 & 1 & 0 & 0 \\ 0.04 & 0 & 0 & -0.0023 \end{bmatrix} \qquad \mathbf{D_o} = \mathbf{0}$$

We will design a stabilizing controller under the architecture shown below.

Figure 26.4: *Optimal quadratic design with integral action*

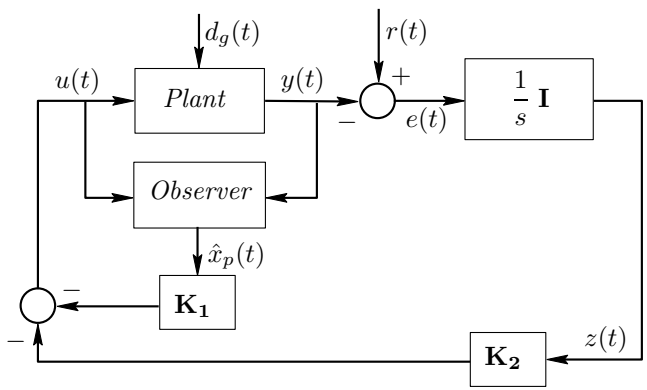

We design an observer for the state $x_p(t)$, given the output $y(t)$. This design uses Kalman-filter theory with $\mathbf{Q} = \mathbf{B_o}\mathbf{B_o}^T$ and $\mathbf{R} = 0.05\mathbf{I}_{2\times 2}$.

The optimal observer gains turn out to be

$$\mathbf{J} = \begin{bmatrix} -3.9272 & 1.3644 \\ 2.6120 & 0.1221 \\ -0.6379 & 0.1368 \\ -2.7266 & -4.6461 \end{bmatrix}$$

We wish to have zero steady-state errors in the face of step input disturbances. We therefore introduce an integrator with transfer function $\mathbf{I}/s$ at the output of the system (*after the comparator*). That is, we add

$$\dot{z}(t) = -y(t) = -\mathbf{C_o} x_p(t)$$

We can now define a composite state vector $\overline{x}(t)=[x_p^T(t)\, z^T(t)]^T$ leading to the composite model

$$\dot{\overline{x}}(t) = \overline{\mathbf{A}}\,\overline{x}(t) + \overline{\mathbf{B}}\,u(t)$$

where

$$\overline{\mathbf{A}} = \begin{bmatrix} \mathbf{A_o} & \mathbf{0} \\ -\mathbf{C_o} & \mathbf{0} \end{bmatrix}; \qquad \overline{\mathbf{B}} = \begin{bmatrix} \mathbf{B_o} \\ \mathbf{0} \end{bmatrix}$$

We next consider the composite system and design a state variable feedback controller via LQR theory.

We choose

$$\mathbf{\Psi} = \begin{bmatrix} \mathbf{C_o}^T\mathbf{C_o} & 0 & 0 \\ 0 & 0.005 & 0 \\ 0 & 0 & 0.1 \end{bmatrix}; \qquad \mathbf{\Phi} = 2\mathbf{I_{2\times 2}}$$

Leading to the feedback gain $\mathbf{K} = [\mathbf{K_1} \quad \mathbf{K_2}]$, where

$$\mathbf{K_1} = \begin{bmatrix} 0.1807 & -0.0177 & 0.1011 & -0.0016 \\ -0.0177 & 0.1496 & 0.0877 & 0.0294 \end{bmatrix}; \qquad \mathbf{K_2} = \begin{bmatrix} 0.0412 & -0.1264 \\ 0.0283 & 0.1844 \end{bmatrix}$$

This leads to the equivalent closed loop shown below (*where we have ignored the observer dynamics, because these disappear in steady state*).

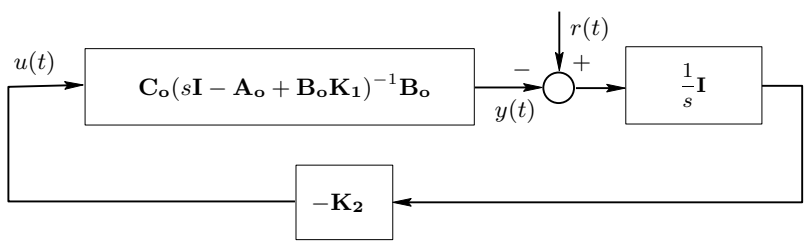

Figure 26.5: *Equivalent closed loop* (ignoring the observer dynamics)

The resulting closed-loop responses for unit step references are shown on the next slide where $r_1(t) = \mu(t - 1)$ and $r_2(t) = -\mu(t - 501)$. Note that, as expected, the system is *statically decoupled*, but significant dynamic coupling occurs during transients, especially following the step in the second reference.

Figure 26.6: *Statically decoupled control*

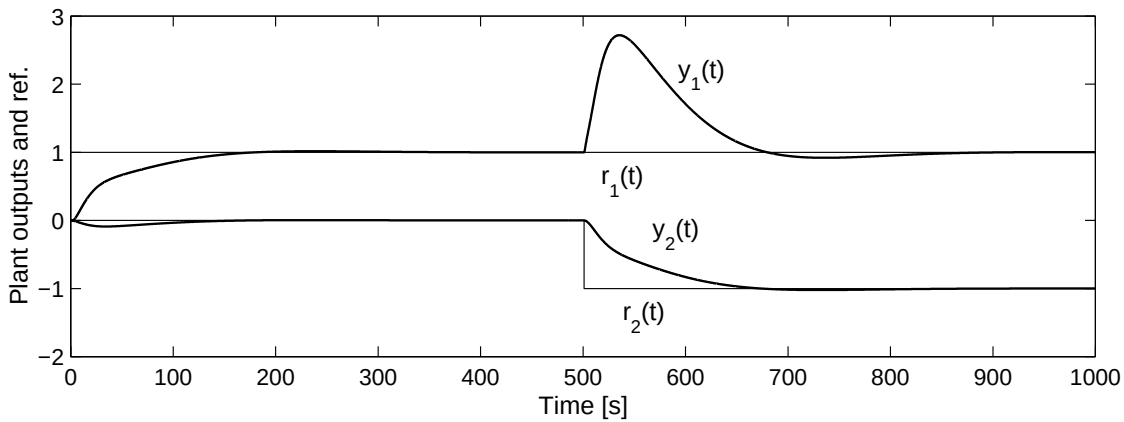

We next design a precompensator to achieve full dynamic decoupling for reference signals. The closed loop has the transfer function

$$\mathbf{T_o}(s) = (\mathbf{I} + \tilde{\mathbf{G}}(s))^{-1}\tilde{\mathbf{G}}(s)$$

where

$$\tilde{\mathbf{G}}(s) = \mathbf{C_o}(s\mathbf{I} - \mathbf{A_o} + \mathbf{B_o}\mathbf{K_1})^{-1}\mathbf{B_o}\mathbf{K_2}\frac{1}{s}$$

This is a stable proper transfer function. Note, however, that this is nonminimum phase, because the original plant was nonminimum phase.

We use the techniques outlined above to design a right inverse that retains dynamic decoupling in the presence of nonminimum-phase zeros. To use those techniques, the equivalent plant is the closed-loop system with transfer function $\tilde{\mathbf{G}}(s) = (\mathbf{I} + \mathbf{G}_o(s))^{-1}\mathbf{G}_o(s)$ and with state space model given by the 4-tuple ($\mathbf{A_e}$, $\mathbf{B_e}$, $\mathbf{C_e}$, 0), where

$$\mathbf{A_e} = \begin{bmatrix} \mathbf{A_o} - \mathbf{B_o}\mathbf{K_1} & \mathbf{B_o}\mathbf{K_2} \\ -\mathbf{C_o} & \mathbf{0} \end{bmatrix}; \quad \mathbf{B_e} = \begin{bmatrix} \mathbf{0} & \mathbf{I} \end{bmatrix}^T; \quad \mathbf{C_e} = \begin{bmatrix} \mathbf{C_o} & \mathbf{0} \end{bmatrix}$$

A suitable interactor for this closed-loop system is

$$\xi_{\mathbf{L}}(s) = \begin{bmatrix} (s+\alpha)^2 & 0 \\ 0 & (s+\alpha)^2 \end{bmatrix}; \quad \alpha = 0.03$$

This leads to an augmented system having the state space model $(\mathbf{A}'_e, \mathbf{B}'_e, \mathbf{C}'_e, \mathbf{D}'_e)$ with

$$\mathbf{A}'_e = \mathbf{A}_e$$
$$\mathbf{B}'_e = \mathbf{B}_e$$
$$\mathbf{C}'_e = \alpha^2 \mathbf{C}_e + 2\alpha \mathbf{C}_e \mathbf{A}_e + \mathbf{C}_e \mathbf{A}_e^2$$
$$\mathbf{D}'_e = \mathbf{C}_e \mathbf{A}_e \mathbf{B}_e$$

The exact inverse then has the state space model $(\mathbf{A}_\lambda, \mathbf{B}_\lambda, \mathbf{C}_\lambda, \mathbf{D}_\lambda)$, where

$$\mathbf{A}_\lambda = \mathbf{A}'_e - \mathbf{B}'_e [\mathbf{D}'_e]^{-1} \mathbf{C}'_e$$
$$\mathbf{B}_\lambda = \mathbf{B}'_e [\mathbf{D}'_e]^{-1} \mathbf{C}'_e$$
$$\mathbf{C}_\lambda = -[\mathbf{D}'_e]^{-1} \mathbf{C}'_e$$
$$\mathbf{D}_\lambda = [\mathbf{D}'_e]^{-1}$$

We now form the two subsystems as described earlier. We form minimal realizations of these two systems, which we denote by ($\mathbf{A_1}$, $\mathbf{B_1}$, $\mathbf{C_1}$, $\mathbf{D_1}$) and ($\mathbf{A_2}$, $\mathbf{B_2}$, $\mathbf{C_2}$, $\mathbf{D_2}$) . We determine stabilizing feedback for these two systems by using LQR theory with

$$\Psi_1 = \mathbf{C}_1^T \mathbf{C}_1 \qquad \Phi_1 = 10^6$$
$$\Psi_2 = \mathbf{C}_2^T \mathbf{C}_2 \qquad \Phi_2 = 10^7$$

We then implement the precompensator as in Figure 26.2, where we choose

$$t_1(s) = \alpha^2 \frac{1 - \mathbf{K}_1 [\mathbf{A}_1]^{-1} \mathbf{B}_1}{(s+\alpha)^2}$$

$$t_2(s) = \alpha^2 \frac{1 - \mathbf{K}_2 [\mathbf{A}_2]^{-1} \mathbf{B}_2}{(s+\alpha)^2}$$

where $\mathbf{K_1}$, $\mathbf{K_2}$ now represent the stabilizing gains for the two subsystems.

The resulting closed-loop responses for step references are shown on the next slide, where $r_1(t) = \mu(\text{t - 1})$ and $r_2(t) = -\mu(\text{t - 501})$. Note that, as expected, the system is now *fully decoupled* from the reference to the output response.

Figure 26.7: *Dynamically decoupled control*

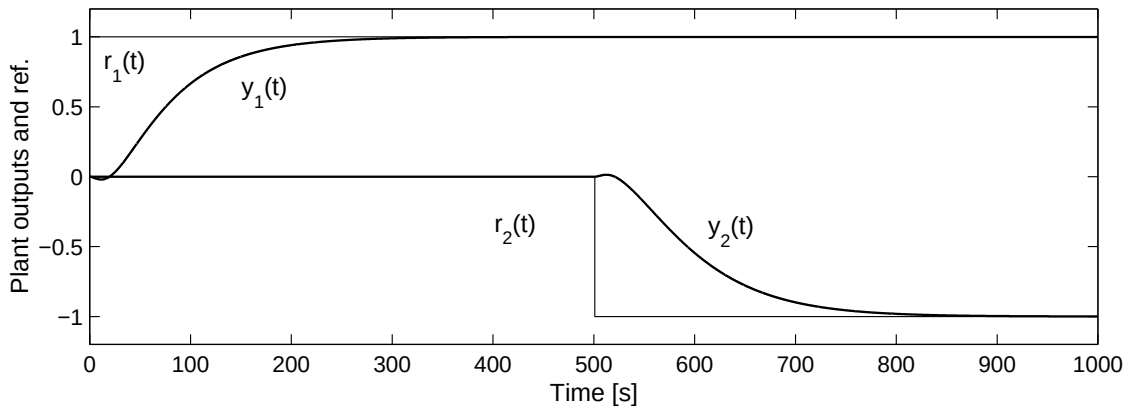

The reader is invited to simulate and study the input/output behavior of the prefilter, $H(s)$. Note the subtly coordinated interaction in the reference signals as seen by the plant (*output of* $H(s)$). It would be virtually impossible for a human operator to manipulate the references, by hand, so that one plant output changed without inducing a transient in the the other output.

Other decoupling designs

It is also possible to obtain the following designs:-

- Two-Degree-of-Freedom Design Based on the Affine Parameterization
- One-Degree-of-Freedom Design using State Feedback

We leave the reader to explore the details in the book.

Zeros of Decoupled and Partially Decoupled Systems

We have seen above that NMP zeros and unstable poles significantly affect the ease with which decoupling can be achieved. Indeed, the analysis above suggests that a single RHP zero or pole might need to be dealt with in multiple loops if decoupling is a design requirement. More details are given in the book.

Frequency-Domain Constraints for Dynamically Decoupled Systems

Further insight into the multivariable nature of frequency-domain constraints can be obtained by examining the impact of decoupling on sensitivity trade-offs.

Consider a MIMO control loop where $\mathbf{S_o}(s)$ and, consequently, $\mathbf{T_o}(s)$ are diagonal stable matrices.

We then have the following theorem which gives an integral constraint on sensitivity when a diagonal decoupling requirement is imposed.

Lemma 26.3: Consider a MIMO plant with a NMP zero at $s = z_0 = \gamma + j\delta$, with associated directions ${h_1}^T$, ${h_2}^T \ldots {h_{\mu_z}}^T$.

Assume, in addition, that $\mathbf{S_o}(s)$ is diagonal; then, for any value of r such that $h_{ir} \neq 0$,

$$\int_{-\infty}^{\infty} \ln|[\mathbf{S_o}(j\omega)]_{rr}| d\Omega(z_o, \omega) = 0; \qquad \text{for} \qquad r \in \nabla_i'$$

Proof: See the book.

Corollary: Under the same hypothesis of the above Lemma, if the MIMO loop is decoupled (*diagonal sensitivity matrix*) and the design specification is $|[\mathbf{S_o}(j\omega)]_{rr}| \leq \epsilon_{rr} << 1$ for $\omega \in [0, \omega_r]$, then

$$||[\mathbf{S_o}(j\omega)]_{rr}||_\infty \geq \left(\frac{1}{\epsilon_{rr}}\right)^{\frac{\psi(\omega_r)}{\pi - \psi(\omega_r)}}$$

Proof: See the book.

We also have the following corresponding result for the complementary sensitivity function.

Lemma 26.4: Consider a MIMO system with an unstable pole located at $s = \eta_0 = \alpha + j\beta$ and having associated directions, $g_1, \ldots, g_{\mu_r}$. Assume, in addition, that $\mathbf{T_o}(s)$ is diagonal; then, for any value of r such that $g_{ir} \neq 0$,

$$\int_{-\infty}^{\infty} \ln|[\mathbf{T_o}(j\omega)]_{rr}| d\Omega(\eta_o, \omega) = 0; \qquad \text{for} \qquad r \in \nabla_i$$

Proof: See the book.

The Cost of Decoupling

We can now investigate the cost of dynamic decoupling, by comparing the results in Chapter 24 with those in the above results. To make the analysis more insightful, we assume that the geometric multiplicity μ_z of the zero is 1 - i.e., there is only one left direction, h_1, associated with the particular zero.

We first assume that the left direction (h_1) has more than one element different from zero - i.e., that the cardinality ∇_i' is larger than one. We then compare the integral constraint applicable in the absence of coupling:

$$\int_{-\infty}^{\infty} \ln |[\mathbf{S_o}(j\omega)]_{rr}| \, d\Omega(z_o, \omega) \geq \int_{-\infty}^{\infty} \ln \left| \frac{h_{ir}[\mathbf{S_o}(j\omega)]_{rr}}{\sum_{k \in \nabla'} h_{ik}[\mathbf{S_o}(j\omega)]_{kr}} \right| d\Omega(z_o, \omega)$$

to the following integral constraint

$$\int_{-\infty}^{\infty} \ln |[\mathbf{S_o}(j\omega)]_{rr}| d\Omega(z_o, \omega) = 0; \qquad \text{for} \qquad r \in \nabla_i'$$

(*applicable to a dynamically decoupled MIMO loop*).

In the first equation, we see that the right-hand side of the inequality can be negative for certain combinations of nonzero off-diagonal sensitivities. Thus, it is feasible to use off-diagonal sensitivities to reduce the lower bound on the diagonal sensitivity peak. This can be interpreted as a two-dimensional sensitivity trade-off, because it involves a spatial as well as a frequency dimension.

We recall that the capacity to use spatial interaction to reduce sensitivity peaks is a feature of MIMO systems. The idea is that *sensitivity dirt* can be shared between outputs. This is shown in cartoon form on the next slide.

Spatial Allocation of Sensitivity

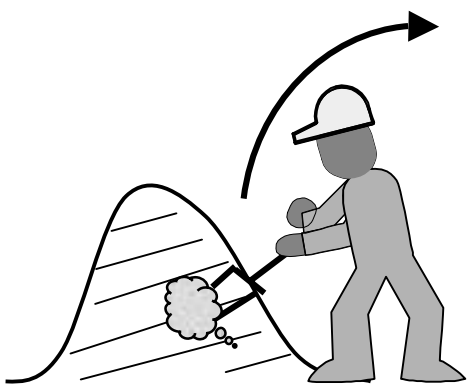

Sensitivity dirt

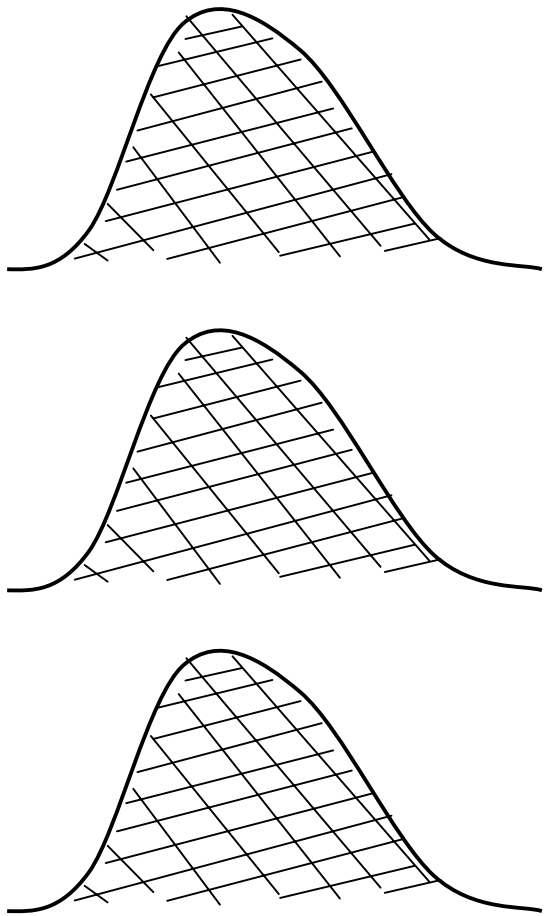

Multiple piles

The conclusion from the above analysis is that it is less restrictive, from the point of view of design trade-offs and constraints, to have an interacting MIMO control loop, compared to a dynamically decoupled one. However, it is a significant fact that to draw these conclusions we relied on the fact that h_1 had more than one nonzero element. If that is not the case, i.e., if only $h_{1_r} \neq 0$ (*the corresponding direction is canonical*), then there is no additional trade-off imposed by requiring a decoupled closed loop.

Example

Consider the following MIMO system:

$$\mathbf{G_o}(s) = \begin{bmatrix} \dfrac{1-s}{(s+1)^2} & \dfrac{s+3}{(s+1)(s+2)} \\ \dfrac{1-s}{(s+1)(s+2)} & \dfrac{s+4}{(s+2)^2} \end{bmatrix} = \mathbf{G_{oN}}(s)[\mathbf{G_{oD}}(s)]^{-1}\mathbf{I}$$

where

$$\mathbf{G_{oN}}(s) = \begin{bmatrix} (1-s)(s+2)^2 & (s+1)(s+2)(s+3) \\ (1-s)(s+2)(s+3) & (s+1)^2(s+4) \end{bmatrix}$$

$$\mathbf{G_{oD}}(s) = (s+1)^2(s+2)^2$$

Zeros

The zeros of the plant are the roots of det($\mathbf{G_{oN}}(s)$) - i.e., the roots of $-s^6 - 11s^5 - 43s^4 - 63s^3 + 74s + 44$. Only one of these roots, namely the one located at s = 1, lies in the RHP. Thus, $z_0 = 1$, and

$$d\Omega(z_o, \omega) = \frac{1}{1+\omega^2} d\omega$$

We then compute $\mathbf{G_o}(1)$ as

$$\mathbf{G_o}(1) = \begin{bmatrix} 0 & \frac{2}{3} \\ 0 & \frac{5}{9} \end{bmatrix}$$

From which it can be seen that the dimension of the null space is $\mu_z = 1$ and the (*only*) associated (*left*) direction is $h^T = [5 \; -6]$.

Clearly, this vector has two nonzero elements, so we could expect that there will be additional design trade-offs arising from decoupling. (*The direction of the RHP zero is not canonical*).

Using the earlier theorem for $r = 1$ and $r = 2$, we obtain, respectively for the non diagonally coupled case:

$$\frac{1}{\pi}\int_{\infty}^{\infty} \ln\left|5[\mathbf{S_o}(j\omega)]_{11} - 6[\mathbf{S_o}(j\omega)]_{21}\right| \frac{1}{1+\omega^2} d\omega \geq \ln(5)$$

$$\frac{1}{\pi}\int_{\infty}^{\infty} \ln\left|5[\mathbf{S_o}(j\omega)]_{12} - 6[\mathbf{S_o}(j\omega)]_{22}\right| \frac{1}{1+\omega^2} d\omega \geq \ln(6)$$

If we impose typical design requirements, we have, for the interacting MIMO loop, that

$$\frac{1}{\pi}\int_{\infty}^{\infty} \ln\left|5[\mathbf{S_o}(j\omega)]_{11} - 6[\mathbf{S_o}(j\omega)]_{21}\right| \frac{1}{1+\omega^2}d\omega \geq \ln(5)$$

$$\frac{1}{\pi}\int_{\infty}^{\infty} \ln\left|5[\mathbf{S_o}(j\omega)]_{12} - 6[\mathbf{S_o}(j\omega)]_{22}\right| \frac{1}{1+\omega^2}d\omega \geq \ln(6)$$

If we require *dynamic decoupling*, the sensitivity integrals become

$$\frac{1}{\pi}\int_{\infty}^{\infty} \ln\left|[\mathbf{S_o}(j\omega)]_{11}\right| \frac{1}{1+\omega^2} d\omega \geq 0$$

$$\frac{1}{\pi}\int_{\infty}^{\infty} \ln\left|[\mathbf{S_o}(j\omega)]_{22}\right| \frac{1}{1+\omega^2} d\omega \geq 0$$

With dynamic decoupling and typical design requirements, we have

$$\left\|[\mathbf{S_o}]_{11}\right\|_\infty \geq \left(\frac{1}{\epsilon_{11}}\right)^{\frac{\psi(\omega_c)}{\pi-\psi(\omega_c)}}$$

$$\left\|[\mathbf{S_o}]_{22}\right\|_\infty \geq \left(\frac{1}{\epsilon_{22}}\right)^{\frac{\psi(\omega_c)}{\pi-\psi(\omega_c)}}$$

To quantify the relationship between the magnitude of the bounds in the coupled and the decoupled situations, we use an indicator κ_{1d}, formed as the quotient between the right-hand sides of inequalities

$$\|[\mathbf{S_o}]_{11}\|_\infty + \frac{6}{5}\|[\mathbf{S_o}]_{21}\|_\infty \geq \left(\frac{1}{\epsilon_{11} + \frac{6}{5}\epsilon_{21}}\right)^{\frac{\psi(\omega_c)}{\pi - \psi(\omega_c)}}$$

$$\|[\mathbf{S_o}]_{22}\|_\infty + \frac{5}{6}\|[\mathbf{S_o}]_{12}\|_\infty \geq \left(\frac{1}{\epsilon_{22} + \frac{5}{6}\epsilon_{21}}\right)^{\frac{\psi(\omega_c)}{\pi - \psi(\omega_c)}}$$

and

$$\|[\mathbf{S_o}]_{11}\|_\infty \geq \left(\frac{1}{\epsilon_{11}}\right)^{\frac{\psi(\omega_c)}{\pi - \psi(\omega_c)}}$$

$$\|[\mathbf{S_o}]_{22}\|_\infty \geq \left(\frac{1}{\epsilon_{22}}\right)^{\frac{\psi(\omega_c)}{\pi - \psi(\omega_c)}}$$

It follows that the indicator of the cost of decoupling is given by:

$$\kappa_{1d} \stackrel{\triangle}{=} \left(1 + \frac{6}{5}\lambda_{1\epsilon}\right)^{-\frac{\psi(\omega_c)}{\pi - \psi(\omega_c)}} \qquad \text{where} \qquad \lambda_{1\epsilon} \stackrel{\triangle}{=} \frac{\epsilon_{21}}{\epsilon_{11}}$$

Thus, $\lambda_{1\,\epsilon}$ is a relative measure of interaction in the direction from channel 1 to channel 2.

The issues discussed above are captured in graphical form in the following figure.

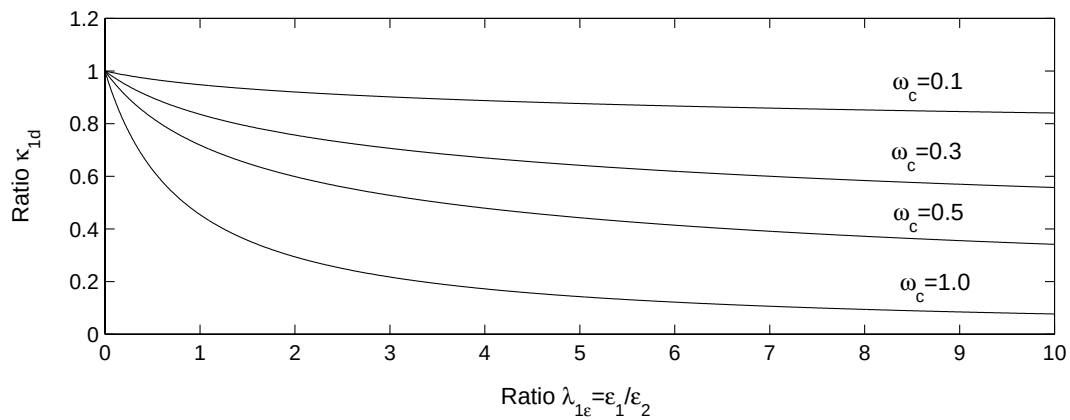

Figure 26.10: *Cost of decoupling in terms of sensitivity-peak lower bounds*

In the above figure, we show a family of curves, each corresponding to a different bandwidth ω_c. Each curve represents, for the specified bandwidth, the ratio between the bounds for the sensitivity peaks as a function of the decoupling indicator, $\lambda_{1\epsilon}$. We can summarize our main observations as follows:

a) When $\lambda_{1\epsilon}$ is very small, there is virtually no effect of channel 1 into channel 2 (*at least in the frequency band* [0, ω_c]); then, the bounds are very close ($\kappa_{1d} \approx 1$).

b) As $\lambda_{1\epsilon}$ increases, we are allowing the off-diagonal sensitivity to become larger than the diagonal sensitivity in [0, ω_c]). The effect of this manifests itself in $\kappa_{1d} < 1$, i.e. in bounds for the sensitivity peak that are smaller than for the decoupled situation.

c) If we keep $\lambda_{1\epsilon}$ fixed and we increase the bandwidth, then the advantages of using a coupled system also grow.

We see, from the above example, that decoupling can be relatively cost-free, depending upon the bandwidth over which one requires that the closed-loop system operate. This is in accord with intuition, because zeros become significant only when one pushes the bandwidth beyond their locations.

We illustrate this conclusion for the system described above.

Consider the plant

$$G(s)=\begin{bmatrix} \frac{1-s}{(s+1)^2} & \frac{s+3}{(s+1)(s+2)} \\ \frac{1-s}{(s+1)(s+2)} & \frac{s+4}{(s+2)^2} \end{bmatrix}$$

which has an ORHP zero at $s = 1$ with output direction equal to $\Psi^* = [5, -6]$.

Since this direction is not canonical, we can argue from the preceding discussion that there will be a cost in sensitivity associated with achieving diagonal decoupling.

If we require $|S_{ik}(j\omega)| \leq \alpha_{ik}$, for ω in $[-\omega_1, \omega_1]$, $i = 1, 2$, then

$$\| S_{11} \|_\infty + \frac{6}{5} \| S_{21} \|_\infty \geq \left(\frac{1}{\alpha_{11} + \frac{6}{5}\alpha_{21}} \right)^{\frac{\Theta_q(\omega_1)}{\pi - \Theta_q(\omega_1)}}$$

Constraints on S_{11} harden as the system is more decoupled.

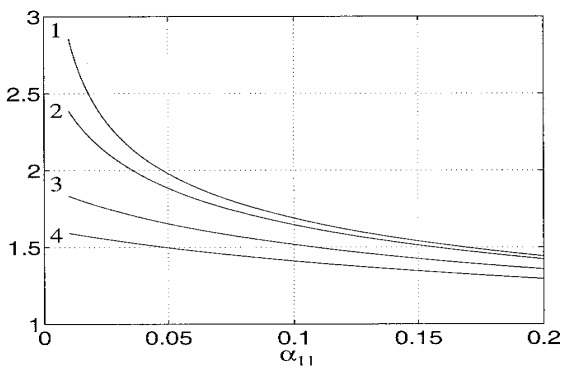

RHS as a function of α_{11}, for $\omega_1 = 0.3$ and for: $\alpha_{21} = 0$, 0.01, 0.05, 0.1 (plots 1 to 4).

We now apply a particular design technique, (*we will not go into details of the design, but* $\lambda = 1$ *gives full dynamic decoupling and* $\lambda = 0$ *gives a triangular design*) that allows different degrees of decoupling while keeping other design parameters essentially constant. The resultant S is

$$S(s) = \begin{bmatrix} \dfrac{s^3 + s^2(2+\lambda) + s(1+3\lambda)}{(s+1)^3} & 0 \\ \dfrac{(\lambda-1)(3s^4 - 16s^3 - 21s^2)}{3(s+1)^5} & \dfrac{s^3 + 3s^2 + 4s}{(s+1)^3} \end{bmatrix}$$

The next slide shows the effect of the extent of decoupling (*measured by* λ) on the magnitude of the sensitivity $S_{11}(j\omega)$.

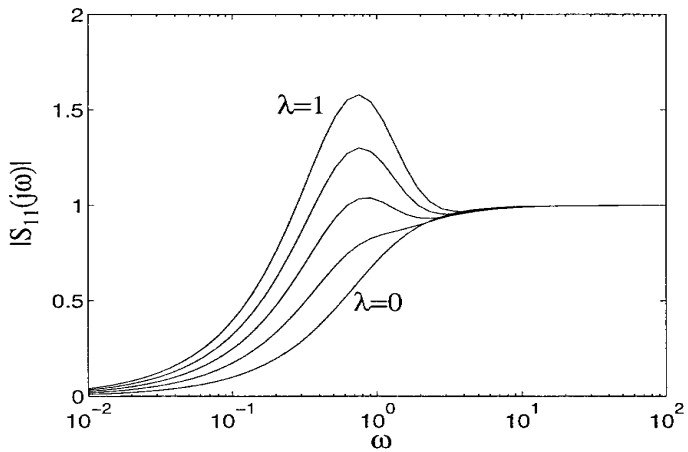

Effect of decoupling on $S_{11}(j\omega)$

We see that the closer we are to full decoupling the greater the peak in sensitivity.

Summary of Cost of Decoupling

- Depending on directionality properties of the zero-pole structure of the plant, design constraints in MIMO may relax with respect to the SISO case (*the cost of ORHP zeros and poles is* distributed *in S or T*).
- If the zero direction is *not* canonical, there is an *additional cost associated to decoupling*, as restrictions concentrate on the diagonal elements.
- If the zero direction is canonical, the system is structurally equivalent to the SISO system, in terms of constraints. There is no additional cost associated with decoupling.

Input Saturation

Finally, we explore the impact that input saturation has on linear controllers that enforce decoupling. We will also develop anti-wind-up mechanisms that preserve decoupling in the face of saturation, using methods that are the MIMO equivalent of the SISO anti-wind-up methods of Chapter 11.

We assume that our plant is modeled as a square system, with input $u(t) \in \mathbb{R}^m$ and output $y(t) \in \mathbb{R}^m$. We also assume that the plant input is subject to saturation. Then if $u^{(i)}(t)$ corresponds to the plant input in the i^{th} channel, $i = 1, 2, \ldots, m$, the saturation is described by

$$u^{(i)}(t) = Sat\langle \hat{u}^{(i)}(t) \rangle \triangleq \begin{cases} u^{(i)}_{max} & \text{if } \hat{u}^{(i)}(t) > u^{(i)}_{max}, \\ \hat{u}^{(i)}(t) & \text{if } u^{(i)}_{min} \leq \hat{u}^{(i)}(t) \leq u^{(i)}_{max}, \\ u^{(i)}_{min} & \text{if } \hat{u}^{(i)}(t) < u^{(i)}_{min}. \end{cases}$$

For simplicity of notation, we further assume that the linear region is symmetrical with respect to the origin, i.e. $|u_{\min}^{(i)}| = |u_{\max}^{(i)}| = u_{sat}^{(i)}$, $i = 1, 2, \ldots, m$. We will describe the saturation levels by $u_{sat} \in \mathbb{R}^m$, where

$$u_{sat} \triangleq \begin{bmatrix} u_{sat}^{(1)} & u_{sat}^{(2)} & \ldots & u_{sat}^{(m)} \end{bmatrix}^T$$

The essential problem with input constraints, as in Chapter 11, is that the control signal can wind up during periods of saturation.

MIMO Anti-Wind-Up Mechanism

In Chapter 11, the wind-up problems were dealt with by using a particular implementation of the controller. This idea can be easily extended to the MIMO case, as follows.

Assume that the controller *transfer-function matrix*, $\mathbf{C}(s)$, is biproper- i.e.,

$$\lim_{s\to\infty}\mathbf{C}(s)=\mathbf{C}_\infty$$

where C_∞ is nonsingular. The multivariable version of the anti-wind-up scheme if as shown on the next slide.

Figure 26.11: *Anti-wind-up controller implementation. MIMO case*

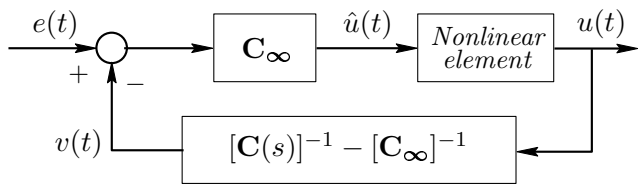

In the scalar case, we found that the nonlinear element could be thought of in many different ways - e.g., as a simple saturation or as a reference governor. However, for SISO problems, all these procedures turn out to be equivalent. In the MIMO case, subtle issues arise from the way that the desired control, $\hat{u}(t)$, is projected into the allowable region. We will explore three possibilities.

(*i*) *simple saturation*

(*ii*) *input scaling*

(*iii*) *error scaling*

Simple saturation: Input saturation is the direct analog of the scalar case.

Input scaling: Here, compensation is achieved by scaling down the controller output vector $\hat{u}(t)$ to a new vector $\beta\hat{u}(t)$, every time that one (or more) component of $\hat{u}(t)$ exceeds its corresponding saturation level. The scaling factor, β, is chosen in such a way that $u(t) = \beta\hat{u}(t)$ - i.e., the controller is forced to come back just to the linear operation zone. This idea is shown schematically below.

Figure 26.12: *Scheme to implement the scaling of controller outputs*

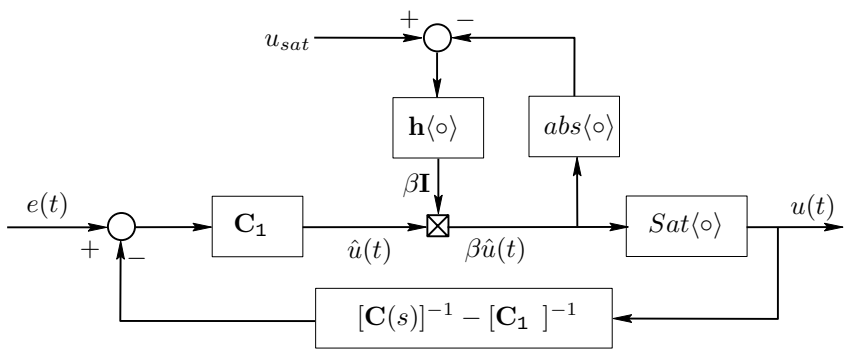

(In the above figure $\mathbf{C}_1$ should be $\mathbf{C}_\infty$)

Error scaling: The third scheme is built by scaling the error vector down to bring the loop just into the linear region. We refer to the following slide.

Figure 26.13: *Implementation of anti-wind-up via error scaling*

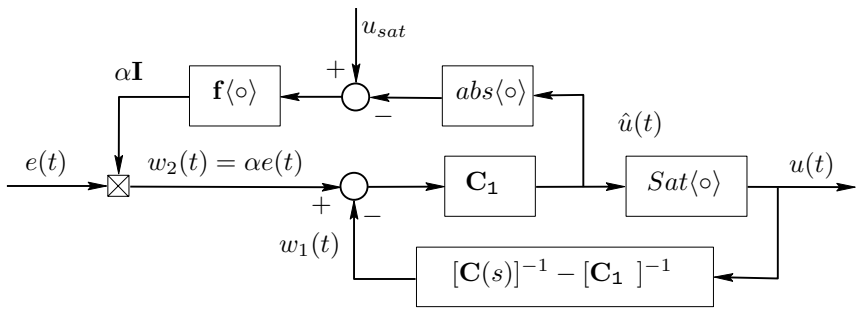

(In the above figure $\mathbf{C}_1$ should be $\mathbf{C}_\infty$)

Note that $\hat{u}$ can be changed only instantaneously by modifying w_2, because $w_1(t)$ is generated through a strictly proper transfer function. Hence, the scaling of the error is equivalent to bringing w_2 to a value such that $\hat{u}$ is just inside the linear region.

In Figure 26.13, the block $f\langle\circ\rangle$ denotes a function that generates the scaling factor $0 < \alpha < 1$. We observe that the block with transfer-function matrix $[\mathbf{C}(s)^{-1}] - \mathbf{C}_\infty$ is strictly proper, so that any change in the error vector $e(t)$ will translate immediately into a change in the vector $\hat{u}(t)$. Instead of introducing abrupt changes in $e(t)$ (and thus in $\hat{u}(t)$, a gentler strategy can be used. An example of this strategy is to generate α as the output of a first-order dynamic system with unit d.c. gain, time constant τ, and initial condition $\alpha(0) = 1$.

Figure 26.14: *Effects of different techniques for dealing with saturation in MIMO systems*

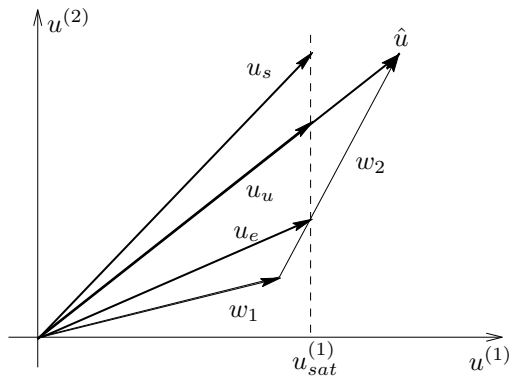

$\hat{u}$: raw control signal

u_s : control signal which results from directly saturating $u^{(1)}$

u_u : control signal obtained with the scaled control technique (*as in Figure 26.12*)

u_e : control signal obtained with the scaled error technique (*as in Figure 26.13*)

Example

Consider a MIMO process having the nominal model

$$\mathbf{G_o}(s) = \frac{1}{(s^2+2s+4)}\begin{bmatrix} -s+2 & 2s+1 \\ -3 & -s+2 \end{bmatrix}$$

with

$$\det(\mathbf{G_o}(s)) = \frac{s^2+2s+7}{(s^2+2s+4)^2}$$

Note that this model is stable and minimum phase. Therefore, dynamic decoupling is possible without significant difficulties.

A suitable decoupling controller is

$$\mathbf{C}(s) = \frac{2(s+2)(s^2+2s+4)}{s(s+1)(s^2+2s+7)} \begin{bmatrix} -s+2 & -2s-1 \\ 3 & -s+2 \end{bmatrix}$$

We first run a simulation that assumes that there is no input saturation. The results are shown below. Observe that full dynamic decoupling has indeed been achieved.

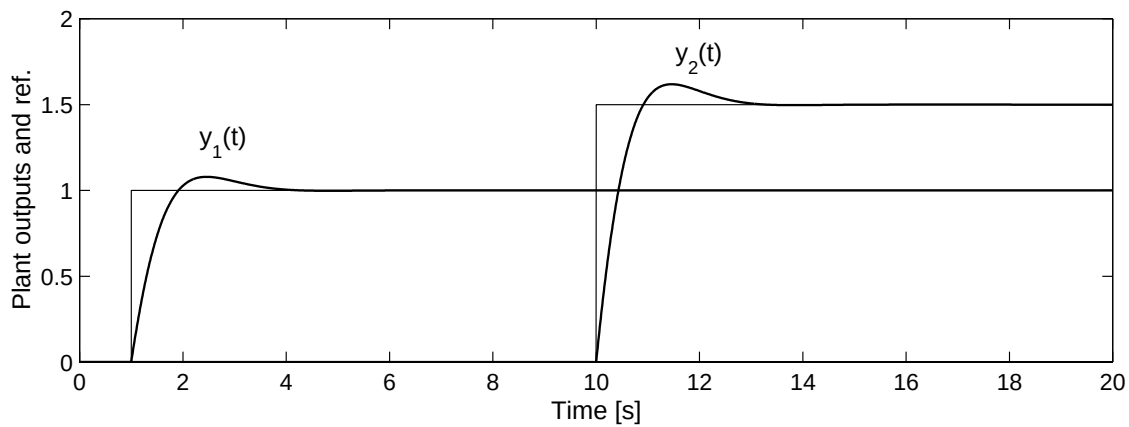

Figure 26.15: *Decoupled design in the absence of saturation*

We run a second simulation including saturation for the controller output in the first channel, at symmetrical levels ±2.5. The results are shown below

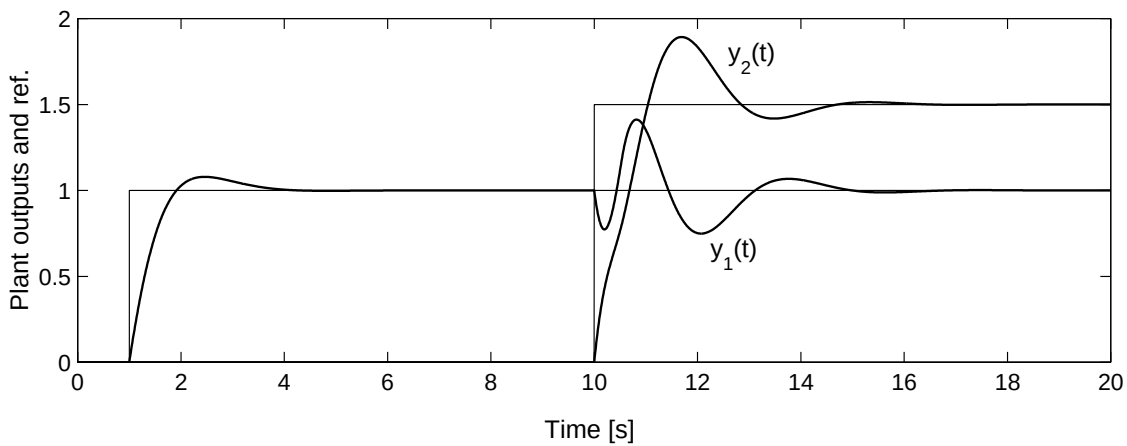

Figure 26.16: *Linear decoupled design - saturation in channel 1, at* ±2.5.

Clearly, the results are very poor. This is due to wind-up effects and stray coupling in the controller that occur during saturation but which have not been compensated. We therefore explore anti-wind-up procedures.

We example the three anti-wind-up procedures described above.

Simple saturation: The results of simply putting a saturation element into the nonlinear element of the MIMO anti-windup current are shown on the next slide. It can be seen that this is unsatisfactory - indeed, the results are similar to those where no anti-wind-up mechanism was used.

Figure 26.17: *Decoupled linear design with saturation in channel 1 and anti-wind-up scheme*

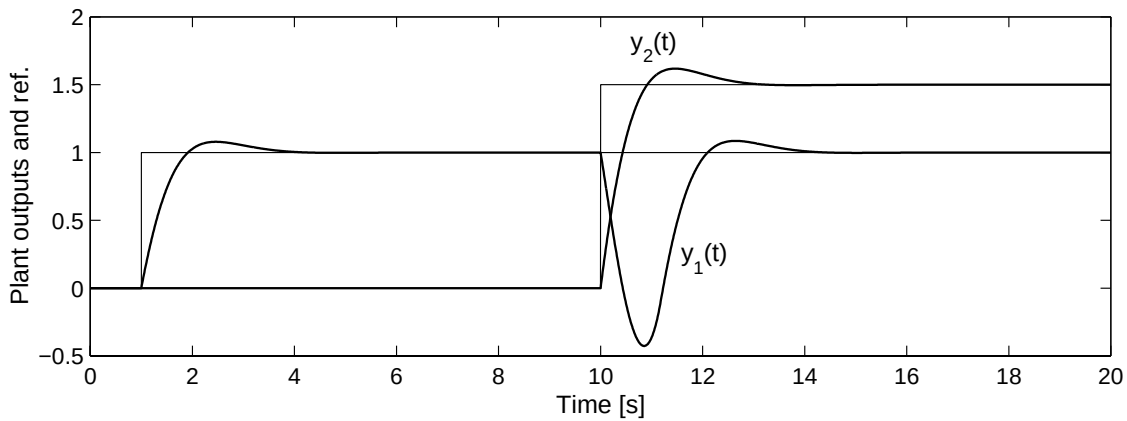

Input scaling: A rather disappointing result is observed regarding the plant outputs. They are shown on the next slide.

The results show only a marginal improvement over those obtained by using the pure anti-wind-up mechanism.

Figure 26.19: *Plant outputs when using control scaling*

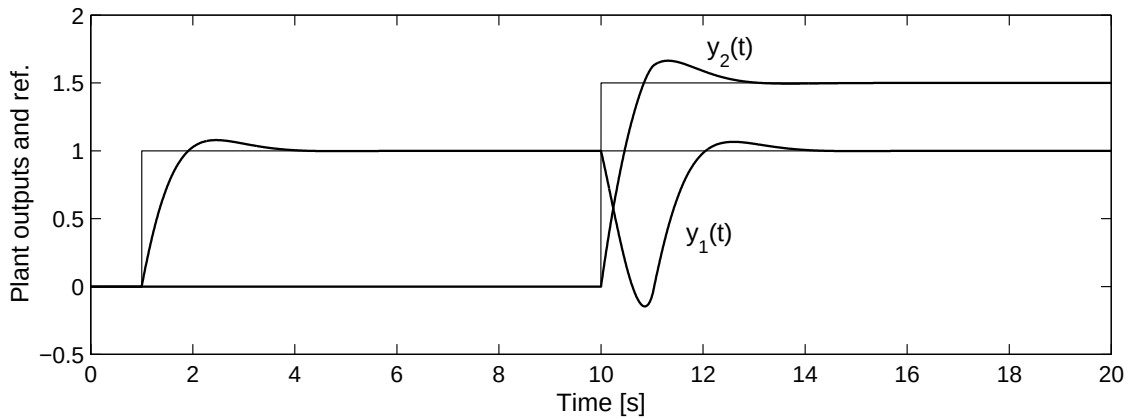

Error scaling: When the error-scaling strategy is applied to our example, we obtain the results shown on the next slide.

Figure 26.20: *Plant outputs when using scaled errors*

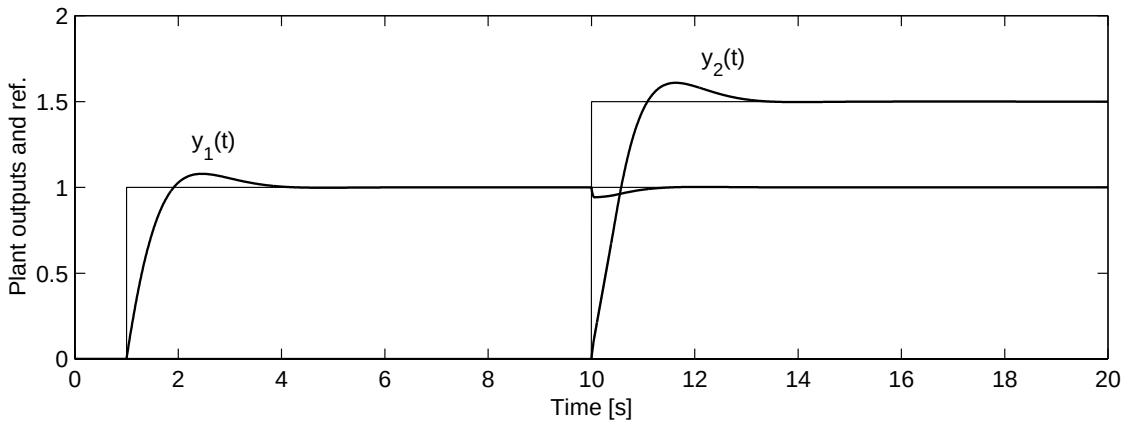

The results are remarkably better than those produced by the rest of the strategies treated so far. Actually, full dynamic decoupling is essentially retained here - the small coupling evident, is due to the implementation of the error scaling via a (*fast*) dynamical system.

Summary

- Recall these key closed-loop specifications shared by SISO and MIMO design:
  - continued compensation of disturbances
  - continued compensation of model uncertainty
  - stabilization of open-loop unstable systems

  whilst not
  - becoming too sensitive to measurement noise
  - generating excessive control signals

  and accepting inherent limitations due to
  - unstable zeros
  - unstable poles
  - modeling error
  - frequency- and time-domain integral constraints

- Generally, MIMO systems also exhibit additional complexities due to
  - directionality (*several inputs acting on one output*)
  - dispersion (*one input acting on several outputs*)
  - and the resulting phenomenon of coupling.
- Designing a controller for closed-loop compensation of this MIMO coupling phenomenon is called *decoupling*.
- Recall that there are different degrees of decoupling, including the following:
  - static (*i.e.,* $\mathbf{T_o}(0)$ *is diagonal*);
  - triangular (*i.e.,* $\mathbf{T_o}(s)$ *is triangular*); and
  - dynamic (*i.e.,* $\mathbf{T_o}(s)$ *is diagonal*).

- Due to the fundamental law that So(s) + To(s) = I, if To exhibits any of these decoupling properties, so does So.
- The severity and types of the trade-offs associated with decoupling depend on
  - whether the system is minimum phase;
  - the directionality and cardinality of nonminimum-phase zeros;
  - unstable poles.
- If all of the system's unstable zeros are canonical (*their directionality affects one output only*), then their adverse effect is not spread to other channels by decoupling, provided that the direction of decoupling is congruent with the direction of the unstable zeros.

- The price for dynamically decoupling a system having noncanonical nonminimum-phase zeros of simple multiplicity is that
  - the effect of the nonminimum-phase zeros is potentially spread across several loops; and,
  - therefore, although the loops are decoupled, each of the affected loops needs to observe the bandwidth and sensitivity limitations imposed by the unstable zero dynamics.
- If one accepts the less stringent triangular decoupling, the effect of dispersing limitations due to nonminimum-phase zeros can be minimized.

- Depending on the case, a higher cardinality of nonminimum-phase zeros can either enforce or mitigate the adverse effects.
- If a system is also open-loop unstable, there may not be any way at all to achieve full dynamic decoupling with a one-d.o.f. controller, although it is always possible with a two-d.o.f. architecture for reference-signal changes.
- If a system is essentially linear but exhibits such actuator nonlinearities as input or slew-rate saturations, then the controller design must reflect this appropriately.

- Otherwise, the MIMO generalization of the SISO wind-up phenomenon can occur.
- MIMO wind-up manifests itself in two aspects of performance degradation:
  - transients due to growing controller states; and
  - transients due to the nonlinearity impacting on directionality.

- The first of these two phenomena …
  - … is analogous to the SISO case.
  - … is due to the saturated control signals not being able to annihilate the control errors sufficiently fast compared to the controller dynamics; therefore the control states continue to grow in response to the nondecreasing control. These wound up states produce the transients when the loop emerges from saturation.
  - … can be compensated by a direct generalization of the SISO anti-wind-up implementation.
- The second phenomena …
  - … is specific to MIMO systems.
  - … is due to uncompensated interactions arising from the input vectors losing its original design direction.

- Analogously to the SISO case, there can be regions in state space from which an open-loop unstable MIMO system with input saturation cannot be stabilized by any control.
- More severely than in the SISO case, MIMO systems are difficult to control in the presence of input saturation, even if the linear loop is stable and the controller is implemented with anti-wind-up. This is due to saturation changing the directionality of the input vector.
- This problem of preserving decoupling in the presence of input saturation can be addressed by anti-wind-up schemes that scale the control *error* rather than the control *signal*.